The remaining 50% of the ligand is distributed among five products. 5,5-Dimethylhydantoin is the major product, and it exhibits a similar wavelength profile as it did in the photolysis of $Cu^{III}(H_{-3}Aib_3a)$ (i.e., forming preferentially from σ-LMCT irradiation). The combination of Aib_2a and its hydrolysis product, Aib_2, accounts for a similar fraction of the total peptide and similar wavelength distribution that Aib_2a did in the photolysis at pH 5. Increasing amounts of **6** with increasing wavelength of irradiation are found, but **7** is not observed at any wavelength. Hydrolysis of **7** is the only mechanism for formation of **6**. Thus, **7** may be present but at the limit of detection. An unknown product, UNK, is observed, and the amount of UNK increases with increasing wavelength. In mobile phase at pH 5.4, UNK has a retention time between those of Aib_3a and Aib_3; at pH 6.2, its retention time decreases slightly and falls between those of Aib_2a and Aib_3. On the basis of its wavelength dependence and the smaller recovery of the 3-substituted hydantoins from cleavage at site A (relative to the H_{-3} form), UNK is believed to form from decomposition of the deprotonated π-aminyl excited state.

Conclusions

The photoredox decomposition of copper(III) peptides is shown to be strongly dependent on the type of donor groups coordinated to the metal. Not only can the trivalent oxidation state of copper be stabilized in aqueous solution toward redox decomposition (in the dark) by coordination to Aib_3a, but in addition the copper(III) peptide can be stabilized toward light-induced redox decomposition by deprotonation of the terminal amine nitrogen. The deprotonated amine complex, $Cu^{III}(H_{-4}Aib_3a)^-$, is significantly less sensitive to UV-vis irradiation than are the other two forms of copper(III)-Aib_3a. The decrease in photoreactivity is attributed to rapid interconversion of the σ- and π-copper(II) amidyl states to the lower energy π-deprotonated aminyl state, which is coupled efficiently to the ground state.

Hydantoins are the principal peptide oxidation products from photolysis of $Cu^{III}(H_{-3}Aib_3a)$ at pH 5 and $Cu^{III}(H_{-4}Aib_3a)^-$ in 1.0 M OH^-. The proposed mechanism for formation of the hydantoins is a novel metal-assisted intramolecular nucleophilic cyclization reaction. This reaction represents an example of an intramolecular nucleophilic reaction where the nucleophile is a metal-coordinated deprotonated peptide (or amide) nitrogen. Hydantoins are not observed in the photolysis of $Cu^{III}(H_{-2}Aib_3a)^+$ in 4.0 M H^+ since dissociation of the ligand fragments and subsequent hydrolysis is more competitive than intramolecular cyclization.

Acknowledgment. This investigation was supported by an Eastman Kodak Industrial Associates Fellowship (J.P.H.) and by Public Health Service Grant No. GM-12152 from the National Institute of General Medical Sciences. The assistance of Kimber D. Fogelman with the pulsed-accelerated-flow studies is greatly appreciated.

Contribution from the Department of Chemistry,
The University of North Carolina, Chapel Hill, North Carolina 27514

Electrochemistry of *trans*-Dioxo Complexes of Rhenium(V) in Water

David W. Pipes and Thomas J. Meyer*

Received February 20, 1986

Cyclic voltammetry of *trans*-$[(py)_4Re^V(O)_2]^+$ (py is pyridine) in aqueous solutions at glassy-carbon electrodes show that oxidation states Re(VI)(d^1) to Re(II)(d^5) are accessible within the solvent limits. Similar behavior is observed for *trans*-$[(CN)_4Re^V(O)_2]^{3-}$ and *trans*-$[(en)_2Re^V(O)_2]^+$. Reduction of the pyridine complex to Re(II) at $0 \le pH \le 14$ leads to H_2; k_{obsd}(room temp, μ = 0.1 M) = 2.4 ($\pm$1.5) $\times 10^{-3}$ s^{-1} at pH 1.2. At pH 6.8 or 13.0, the addition of NO_2^- or SO_3^{2-} suppresses water reduction at the expense of electrocatalytic reduction of NO_2^- to NH_3 and N_2O and of SO_3^{2-} to H_2S or HS^-. Comparisons between the Re-pyridyl-based couples and the structurally and electronically related *trans*-$[(bpy)_2Os^{VI}(O)_2]^+$ (bpy is 2,2'-bipyridine) couples suggest that the pattern of couples that appear and their pH dependences are determined largely by the d-electronic configurations of the components. Differences in the magnitudes of redox potentials between electronically equivalent Re and Os couples are determined by the differences in oxidation state between the two types of couples.

Introduction

The higher oxidation state oxo complexes of Os and Ru have a rich chemistry as oxidants in reactions as diverse as the oxidation of alcohols to ketones,[1] alllylic C-H groups to carboxylates,[1] phenols to quinones,[2] NO_2^- to NO_3^-,[3] olefins to epoxides,[4] HCO_2^- to CO_2,[5] H_2O to O_2,[6] and Cl^- to Cl_2.[7] The higher oxidation states are stabilized by metal-oxo formation following oxidative deprotonation of aqua or hydroxo groups, e.g.

$$[(bpy)_2(py)Ru^{II}\text{—}OH_2]^{2+} \xrightarrow[-H^+]{-e^-}$$

$$[(bpy)_2(py)Ru^{III}\text{—}OH]^{2+} \xrightarrow[-H^+]{-e^-} [(bpy)_2(py)Ru^{IV}\text{=}O]^{2+}$$ [8a,b]

(bpy is 2,2'-bipyridine; py is pyridine). Stabilization by oxo groups lowers the redox potentials for couples involving higher oxidation states to such a degree that extended series of redox couples are accessible within the solvent limits. For example, potentials for Os(VI/V), Os(V/IV), Os(IV/III), and Os(III/II) couples based on *cis*-$[(bpy)_2Os^{II}(OH_2)_2]^{2+}$ and *cis*-$[(bpy)_2Os^{VI}(O)_2]^{2+}$ occur over a potential range of only 0.7 V at pH 4.[8c,d]

For the Ru and Os complexes as stoichiometric or catalytic oxidants the important feature is the accessibility of higher oxidation state oxo complexes. For Mo, W, and Re in equivalent coordination environments and oxidation states, the metals are more electron-rich and higher oxidation states are the norm as metal-oxo complexes. However, for these metals the possibility exists that, upon reduction and protonation, aqua or hydroxo

(1) (a) Moyer, B. A.; Thompson, M. S.; Meyer, T. J. *J. Am. Chem. Soc.* **1978**, *102*, 2310. (b) Thompson, M. S.; DeGiovani, W. F., Moyer, B. A.; Meyer, T. J. *J. Org. Chem.* **1984**, *25*, 4972.
(2) Roecker, L. Ph.D. Dissertation, The University of North Carolina, Chapel Hill, NC, 1985.
(3) (a) Moyer, B. A.; Meyer, T. J. *J. Am. Chem. Soc.* **1979**, *101*, 1326. (b) McGuire, M., work in progress.
(4) Dobson, J.; Seok, W.; Meyer, T. J. *Inorg. Chem.* **1986**, *25*, 1513.
(5) Roecker, L.; Meyer, T. J. *J. Am. Chem. Soc.*, in press.
(6) (a) Gersten, S. W.; Samuels, G. J.; Meyer, T. J. *J. Am. Chem. Soc.* **1982**, *104*, 4029. (b) Goswanai, S.; Chakravorty, A. R.; Chakravorty, A. *J. Chem. Soc., Chem. Commun.* **1982**, 1288. (c) Gilbert, J. A.; Eggleston, D. S.; Murphy, W. R., Jr.; Geselowitz, D. A.; Gersten, S. W.; Hodgson, D. J.; Meyer, T. J. *J. Am. Chem. Soc.* **1985**, *107*, 3855-3864. (d) Honda, K.; Frank, A. J. *J. Chem. Soc., Chem. Commun.* **1984**, 1436. (e) Collin, J. P.; Sauvage, J. P. *Inorg. Chem.* **1986**, *25*, 135.
(7) (a) Ellis, C. D.; Gilbert, J. A.; Murphy, W. R., Jr.; Meyer, T. J. *J. Am. Chem. Soc.* **1983**, *105*, 4842. (b) Vining, W. J.; Meyer, T. J. *Inorg. Chem.* **1986**, *25*, 2015.
(8) (a) Moyer, B. A.; Meyer, T. J. *Inorg. Chem.* **1981**, *20*, 436. (b) Moyer, B. A.; Meyer, T. J. *J. Am. Chem. Soc.* **1978**, *100*, 3601. (c) Takeuchi, K. J.; Samuels, G. J.; Gersten, S. W.; Gilbert, J. A.; Meyer, T. J. *Inorg. Chem.* **1983**, *22*, 1407. (d) Dobson, J. C.; Takeuchi, K. J.; Pipes, D. W.; Geselowitz, D. A.; Meyer, T. J. *Inorg. Chem.* **1986**, *25*, 2357. (e) Che, C.-M.; Tang, T.-W.; Poon, C. K. *J. Chem. Soc., Chem. Commun.* **1984**, 641.

0020-1669/86/1325-3256$01.50/0

complexes may be reached that are capable of acting in the opposite sense, as stoichiometric or catalytic reductants, as shown, for example, for $[(cat)_2Mo^{VI}(O)_2]^{2-}$ by Lahr, Finklea, and Schultz[9] (cat = catecholate).

Although an extended series of Re(V)–oxo and –dioxo complexes exists that are stable in the solid state and in solution, e.g., $[(PPh_3)_2(Cl)_3Re^{V}{=}O]$, $[(CN)_4Re^{V}(O)_2]^{3-}$, $[(en)_2Re^{V}(O)_2]^{+}$, *trans*-$[(py)_4Re^{V}(O)_2]^{+}$, and $(sal_2phen)_2Re_2^{V}(O)_3$((sal)$_2$phen is *N,N'-o*-phenylenebis(salicylideneaminate) anion, en is ethylenediamine, and py is pyridine),[10-12] little is known about their aqueous solution electrochemistry.

We report here our results on the aqueous solution electrochemistry of *trans*-$[(py)_4Re^{V}(O)_2]^{+}$. Our goals were to acquire sufficient data to be able to make quantitative comparison between Re and related complexes of Os or Ru and to explore the possible development of aqua–Re(III)- or aqua–Re(II)-based reductive electrocatalysts. The X-ray crystal structure of *trans*-$[(py)_4Re^{V}(O)_2](Cl)\cdot 2H_2O$ shows that the complex has the *trans*-dioxo structure (Re=O = 1.76 (3) Å) with four pyridine ligands bound in the equatorial plane.[13] In the structure the pyridine groups are tilted at angles of 10–20° with respect to the equatorial plane. From the results of solution studies the oxo groups are known to protonate in acidic solution to yield $[(py)_4Re^{V}(O)(OH)]^{2+}$ and $[(py)_4Re^{V}(OH)_2]^{3+}$, and in 1.0 M HCl, slow loss of pyridine occurs (~10 h), yielding $[(py)_2(Cl)_2Re^{V}(O)(OH)]$ and, in more concentrated HCl, $[(py)_2(Cl)_2Re^{V}(OH)_2](Cl)$.[11a]

Experimental Section

Materials. $KReO_4$, triphenylphosphine, and trifluoromethanesulfonic acid (HSO_3CF_3, (TFMS)H), obtained from Aldrich Chemical Inc., and sodium nitrite and sodium sulfite, obtained from Fisher Scientific Co., were used without further purification. All other chemicals were reagent grade and also used without further purification.

Measurements. Ultraviolet and visible spectra were obtained in quartz cells with a Bausch & Lomb Spectronic 210 UV 2000 spectrophotometer. Spectroelectrochemical experiments were carried out in a three-compartment cell where the working-electrode compartment was a quartz cuvette. Due to the reducing nature of the electrogenerated species, all compartments were deaerated with argon and sealed with rubber septa. Kinetics data were taken with a Gilford 240 UV–vis spectrophotometer with absorbance vs. time curves recorded on a Varian Model 9176 strip-chart recorder. Infrared spectra were obtained as KBr pellets with a Nicolet Model 20DX FTIR instrument Cyclic voltammograms in aqueous solutions were obtained at a Tokai glassy-carbon working electrode[14] vs. the saturated sodium chloride calomel reference electrode (SSCE). A Pt wire was used as the auxiliary electrode. For coulometric experiments either a mercury pool or a piece of shaped reticulated vitreous carbon[14] was used as the working electrode with a copper-wire connection. For coulometric studies, a gastight cell equipped with gas and liquid sampling ports was used or, if gas sampling was not required, a simple H-cell sealed with septa was used with continuous flushing with an inert gas. Potentials in coulometric experiments were applied with a PAR 173 galvanostat potentiostat, and the electrical equivalents were measured with a PAR 179 digital coulometer. Cyclic voltammograms were obtained with a PAR 173 galvanostat potentiostat connected to a Supercycle[15] or a PAR 175 universal programmer. Gas–liquid chromatographic analysis of the products obtained by coulometric reduction of H_2O or NO_2^- in aqueous solution by Re(II) was performed with a Hewlett-Packard Model 5894 GLC. A 5A molecular sieve column with argon as the carrier gas was used for hydrogen analysis, and a Chromasorb 103 stainless steel column with helium as the carrier gas was used for NH_3 or N_2O. A thermal conductivity detector (TCD) was used in either case.

Preparations. Literature procedures were used to prepare the complexes *trans*-$[(py)_4Re(O)_2](Cl)$,[11b] $[(en)_2Re(O)_2](ClO_4)$,[11b] and $K_3[(CN)_4Re(O)_2]$.[10b]

***trans*-$[(py)_4Re(O)_2](ClO_4)$.** The Cl^- salt of the complex (0.2 g) was dissolved in the minimum amount of H_2O (10 mL) and filtered through a medium frit. To the filtrate was added 1 mL of saturated $NaClO_4$ solution, which was then cooled to 5 °C for 1 h. The precipitate formed was filtered, washed two times with H_2O, and dried in a vacuum desiccator. Anal. Calcd: C, 37.88; H, 3.19; N, 8.84; Cl, 5.59. Found: C, 38.06; H, 3.20; N, 8.87; Cl, 5.08.

Electrochemistry. Product Analysis in the Reduction of H_2O by Re(II). In the reduction of H_2O to H_2, 6–25 mg of $[(py)_4Re^{V}(O)_2](ClO_4)$ was dissolved in 25 mL of aqueous solution, with μ = 0.1 M at pH 1.2 (0.1 M in trifluoromethanesulfonic acid (TFMS)H)), at pH 6.8 (sodium phosphate buffer), or at pH 13 (0.1 M NaOH), and deaerated with argon in the gastight electrochemical cell. A mercury-pool working electrode was used to apply the potentials, E_{app} = –0.87 V vs. SSCE at pH 1.2, E_{app} = –1.40 V at pH 6.8, and E_{app} = –1.55 V at pH 13, sufficiently reducing to generate Re(II). Cyclic voltammograms were taken before and after the bulk coulometric experiments with use of glassy-carbon electrodes to check catalyst stability. The electrical equivalents were measured at time periods ranging from 20 min to 2 h, and the gas in the cell was sampled (5–20 μL) every 20 min until termination of the experiment. The reduction product, hydrogen, was verified by comparison to H_2 standards and quantitative measurements made by comparisons to a calibration curve made by injecting known amounts of H_2 into the GC and measuring the peak areas. The H_2 standards were made by deaerating a sealed vial of known volume with argon and injecting 0.100–0.700 mL of H_2 into the vial. Gas samples ranging from 10 to 20 μL were taken from the vial and injected into the GC.

Kinetics of the Reduction of H_2O by $(py)_4Re^{II}(OH_2)_2^{2+}$ at pH 1.2. In the kinetic runs the concentration of $[(py)_4Re^{V}(O)_2](ClO_4)$ was varied from 8.2×10^{-5} to 1.2×10^{-4} M in 0.1 M trifluoromethanesulfonic acid (pH 1.2). Solutions containing $[(py)_4Re^{II}(OH_2)_2]^{2+}$ were prepared under N_2 or Ar in a spectroelectrochemical cell from $[(py)_4Re^{V}(O)_2]^{+}$ at a reticulated-vitreous-carbon or mercury-pool electrode at a potential of –0.87 V vs. SSCE or by stirring the solution over excess Zn(Hg). Absorbance spectral changes from 600 to 350 nm were followed immediately after generation of Re(II). The loss of absorbance at λ_{max} = 458 nm for $[(py)_4Re^{II}(OH_2)_2]^{2+}$ was followed for time periods of 10–15 min ($2^1/_2$–3 half-times). The data were analyzed on the assumption of first-order kinetics in Re(II). Correlation coefficients of 0.999 or greater were obtained for least-squares fits of log $(A - A_\infty)$ vs. time, where A is the absorbance at time t and A_∞ is that at $t = \infty$. An average rate constant of $k_{obsd} = 2.4\ (\pm 1.5) \times 10^{-3}\ s^{-1}$ was found for 10 kinetic runs.

Electrocatalytic Reduction of NO_2^- and SO_3^{2-} by Re(II). The same electrochemical cell and procedure used for the reduction of H_2O was used for the reduction of NO_2^- and SO_3^{2-}. Because of sizable backgrounds in acidic solution because of H_2 production, the electrocatalytic experiments were carried out at pH 6.8 and 13. The solutions were made 0.1 M in $NaNO_2$ or Na_2SO_3. Solutions were electrolyzed at potentials sufficiently reducing to generate Re(II), and electrolysis periods were for 20 min to 2 h. Solutions initially containing NO_2^- were analyzed for NH_3 by GLC by injecting 2–10 μL of the aqueous solution into a 3-ft Chromasorb 103 stainless steel column, equipped with a 3-in. precolumn to remove excess salts. The oven temperature was 125 °C, and the helium gas flow rate was 0.3–0.4 mL/s. Analysis for sulfide, the product of SO_3^{2-} reduction, was carried out by qualitative methods relying on simple chemical tests. Any combination of sulfide, hydrosulfides, and metal sulfides were detected by adding to a $^1/_2$-mL sample of the electrolyzed solution several drops of NaN_3/I_2 solution, which catalytically produces N_2 in the presence of S^{2-}. This test is good in the presence of SO_3^{2-} or SO_4^{2-}.[16] In addition, the addition of a drop of an aqueous Cd^{2+} solution produces a bright yellow precipitate of CdS. The electrocatalytic reduction of SO_3^{2-} was not investigated quantitatively since the catalyst is destroyed as S^{2-} builds up in the solution.

Results

Electronic Spectra. The electronic spectrum of d^2 *trans*-$[(py)_4Re^{V}(O)_2]^{+}$ has been studied in aqueous solution[11a] and recently in a single crystal.[11c] In aqueous solution bands appear at λ_{max} = 445 nm (ϵ = 1200 $M^{-1}\ cm^{-1}$) and λ_{max} = 331 nm (ϵ = 19 400 $M^{-1}\ cm^{-1}$). In the crystal a shoulder also appears at λ =

(9) Lahr, S. K.; Finklea, H. O.; Schultz, F. A. *J. Electroanal. Chem. Interfacial Electrochem.* **1984**, *163*, 237.
(10) (a) Johnson, N. P.; Lock, N. P.; Wilkinson, G. *Inorg. Synth.* **1967**, *9*, 145. (b) Lock, C. J. N.; Wilkinson, G. *J. Chem. Soc.* **1964**, 2281.
(11) (a) Beard, J. H.; Casey, J.; Murmann, R. K. *Inorg. Chem.* **1965**, *4*, 797. (b) Johnson, N. P.; Lock, C. N.; Wilkinson, G. *J. Chem. Soc.* **1964**, 1054. (c) Winkler, J. R.; Gray, H. B. *Inorg. Chem.* **1985**, *24*, 346.
(12) Middleton, A. R.; Masters, A. F.; Wilkinson, G. *J. Chem. Soc., Dalton Trans.* **1979**, 542.
(13) Calvo, C.; Krishnamachari, N.; Lock, C. J. L. *J. Cryst. Mol. Struct.* **1971**, *1*, 161.
(14) (a) Tokai carbon was obtained from Tokai Chemical Co., Tokyo, Japan. (b) Reticulated vitreous carbon was obtained from Chemtronics International, Inc., Ann Arbor, MI 48104 (313-971-4060).
(15) Woodward, W. S.; Rocklin, R. D.; Murray, R. W. *Chem., Biomed. Environ. Instrum.* **1979**, *9*, 95.
(16) Feigel, F., Anger, V. *Spot Tests in Inorganic Chemistry*; Elsevier: New York, 1972; p 437.

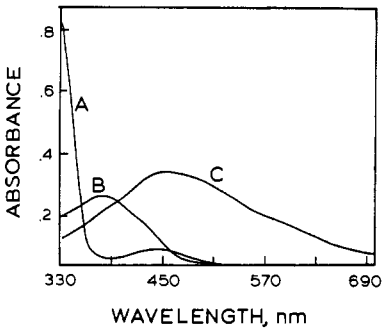

Figure 1. Visible spectra in 0.1 M (TFMS)H (HSO_3CF_3) of 4.1×10^{-5} M aqueous solutions (1-cm path length): (A) *trans*-$[(py)_4Re^{V}(O)_2]^+$; (B) $[(py)_4Re^{III}(OH)(OH_2)]^{2+}$; (C) $[(py)_4Re^{II}(OH_2)_2]^{2+}$.

Table I. Visible Spectra of Re Complexes in Aqueous Solutions (λ_{max} in nm, ϵ in M^{-1} cm^{-1})[a]

complex	λ_{max} (ϵ)
pH 1.2–13.0	
trans-$[(py)_4Re^{V}(O)_2]^+$	445 (1200)
	331 (19 400)
pH 1.2	
$[(py)_4Re^{III}(OH)(OH_2)]^{2+}$	435 sh
	383 (6300)
$[(py)_4Re^{II}(OH_2)_2]^{2+}$	598 sh
	458 (8600)
pH 3.0	
$[(py)_4Re^{III}(OH)_2]^+$	387 (10 000)
$[(py)_4Re^{II}(OH_2)_2]^{2+}$	458
pH 6.8	
$[(py)_4Re^{III}(O)(OH)]$	409 (11 000)
$[(py)_4Re^{II}(OH)(OH_2)]^+$	*b*
pH 13.0	
$[(py)_4Re^{III}(O)(OH)]$	409 (11 000)
$[(py)_4Re^{II}(O)(OH)]^-$	~466[b]

[a] The pH contents of the various complexes were deduced from pH-dependent electrochemical studies. Acquisition of spectral data for Re(II) is complicated by the reduction of H_2O to H_2. [b] Oxidation of Re(II) by H_2O at pH 6.8 was too rapid to obtain the spectrum of Re(II). Both Re(III) and Re(II) were present in the solution.

485 nm (ϵ = 50 M^{-1} cm^{-1}). In concentrated HCl, where $[(py)_4Re^{V}(O)(OH)]^{2+}$ is the dominant form, λ_{max} = 504 nm (ϵ = 540 M^{-1} cm^{-1}), and λ_{max} = 297 nm. In concentrated H_2SO_4, where $[(py)_4Re^{V}(OH)_2]^{3+}$ is the dominant form, λ_{max} = 605 nm. The band at λ = 331 nm can probably be assigned to a $\pi^*(py) \leftarrow d\pi(Re^{V})$ transition on the basis of the shift to higher energy that occurs upon protonation in acidic solutions. The band at λ = 445 nm and the shoulder at λ = 485 nm have been assigned as d ← d singlet–singlet and single–triplet transitions.[11c] Crystals of *trans*-$[(py)_4Re^{V}(O)_2](BF_4)$ emit strongly via a d–d luminescence with lifetimes of 32–60 μs from 30 to 300 K, but the emission is completely quenched in aqueous solutions.[11c]

The UV–visible spectrum of *trans*-$[(py)_4Re^{V}(O)_2]^+$ is shown in Figure 1 at pH 1.2. Reduction to d^4 $[(py)_4Re^{III}(OH)(OH_2)]^{2+}$ gives λ_{max} = 383 nm (ϵ = 6300 M^{-1} cm^{-1}). The proton content of the Re(III) complex in acidic solution is based on the analysis of pH-dependent electrochemical data given below. Further reduction to d^5 $[(py)_4Re^{II}(OH_2)_2]^{2+}$ gives a band at λ_{max} = 458 nm (ϵ = 8600 M^{-1} cm^{-1}) and a shoulder at λ = 598 nm with an isosbestic point appearing at λ = 398 nm between the Re(III) and Re(II) complexes. The spectrum shown in Figure 1 for Re(II) represents a lower limit of its absorptivity because of the relatively rapid reduction of H_2O to H_2 by Re(II) (see below).

A summary of the absorption spectra for Re(V), Re(III), and Re(II) as a function of pH is given in Table I. The intense visible bands that appear for both Re(II) and Re(III) may arise from $\pi^*(py) \leftarrow d\pi(Re)$ metal to ligand charge-transfer (MLCT) transitions. The shifts to lower energy as the complexes are deprotonated are consistent with this assignment. For aqua polypyridyl complexes of Ru and Os, deprotonation at the aqua ligand to give hydroxo complexes destabilizes the $d\pi$ levels and causes a shift to lower energy for MLCT transitions.[8,17] For example, for $[(trpy)(bpy)Os^{II}OH_2^{2+}]$ (trpy = 2,2′:6′,2″-terpyridine) λ_{max} = 499 nm and for $[(trpy)(bpy)Os^{II}OH]^+$ λ_{max} = 520 nm.[17] However, the spectral manifolds are complex and may include contributions from additional MLCT bands or LMCT $d\pi(Re) \leftarrow p^*(OH^-)$ bands on the basis of comparisons with related complexes of Re(II) and Re(III) that do not have pyridine ligands.[18]

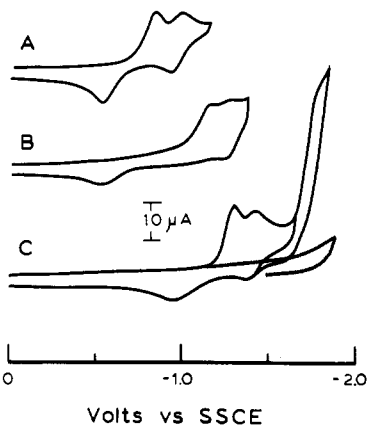

Figure 2. Cyclic voltammograms (100 mV/s) of *trans*-$[(py)_4Re^{V}(O)_2]^+$ in aqueous solutions with glassy-carbon working electrodes vs. SSCE: (A) pH 4.0 (μ = 0.1 M (acetate)); (B) pH 6.8 (μ = 0.1 M (phosphate)); (C) pH 12.7 (μ = 0.1 M (NaOH)).

Electrochemistry of *trans*-$[(py)_4Re^{V}(O)_2]^+$ in Aqueous Solution. A cyclic voltammogram of *trans*-$[(py)_4Re^{V}(O)_2]^+$ in 0.1 M (TFMS)H at a glassy-carbon working electrode is shown in Figure 2. An oxidative wave (not shown) is observed at $E_{1/2}$ = 1.25 V vs. SSCE for the Re(VI/V) couple, which by coulometry is a one-electron couple (n = 1.0 ± 0.2). However, although the Re(VI/V) couple is reversible on the CV time scale (100 mV/s), on the longer time scale for coulometry decomposition occurs, yielding an unidentified product.

Scanning in the reductive direction gives first a multielectron wave at $E_{1/2}$ = –0.43 V, which by coulometry using a mercury-pool working electrode gave n = 2.0 (±0.2), suggesting a Re(V/III) couple. The large peak to peak splitting, $\Delta E_p = E_{p,a} - E_{p,c}$ = 240–340 mV at sweep rates of 20–200 mV/s, indicates that the couple is electrochemically quasi-reversible. Reoxidation of Re(III) back to Re(V) (n = 2.0 ± 0.4) shows that the couple is chemically reversible. At more negative potentials, a reversible wave (ΔE_p = 60 mV) appears at $E_{1/2}$ = –0.75 V. Determination of n for the couple by coulometry was difficult because of the reduction of H_2O to H_2 following reduction. However, with use of a large-surface-area mercury-pool electrode and short electrolysis times a value of n = 1.0 (±0.4) was established, consistent with the reduction of Re(III) to Re(II).

As shown in Figure 2, the Re(V/III) and Re(III/II) couples are pH-dependent. The Pourbaix diagram in Figure 3 shows how the $E_{1/2}$ values for the various couples vary with pH. In the diagram the dominant oxidation state in a given pH–potential domain is shown at the right. The proton compositions of the various oxidation states are indicated by the oxo, hydroxo, and aqua symbols in the diagram. For example, in the pH region 0 < pH < 2.2, the dominant forms of the complex in oxidation states VI, V, III, and II are $[(py)_4Re^{VI}(O)_2]^{2+}$, $[(py)_4Re^{V}(O)_2]^+$, $[(py)_4Re^{III}(OH)(OH_2)]^{2+}$, and $[(py)_4Re^{II}(OH_2)_2]^{2+}$. The proton compositions of the complexes were determined by comparing the slopes of the $E_{1/2}$ vs. pH plot to expected values calculated from the Nernst equation in the form $E_{1/2} = E_{1/2}^{\circ} - (0.059m/n)$pH.

(17) Takeuchi, K. J.; Thompson, M. S.; Pipes, D. W.; Meyer, T. J. *Inorg. Chem.* **1984**, *23*, 1845.
(18) Leigh, G. J.; Mingos, D. M. P. *J. Chem. Soc. A* **1970**, 587.

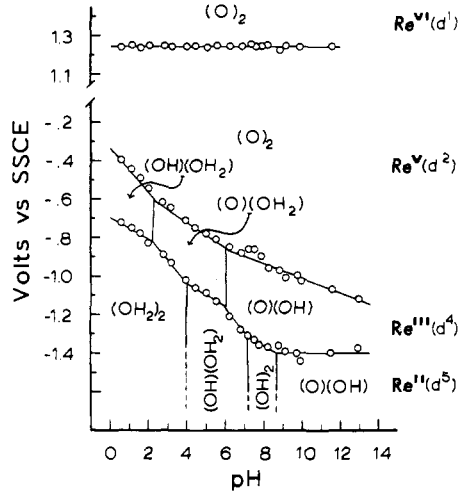

Figure 3. $E_{1/2}$ vs. pH (Pourbaix) diagram for *trans*-$[(py)_4Re^{V}(O)_2]^+$ using a mixture of normal and activated[20] glassy-carbon working electrodes vs. SSCE over the pH range 0.5–13 (μ = 0.1 M).

In the equation *m* is the number of protons gained in the half-cell reduction and *n* is the number of electrons gained. $E_{1/2}°$ is the half-wave potential at pH 0. For example, a slope of −59 mV/pH unit occurs for couples where the ratio of electrons to protons is 1/1: 1 e^-/1 H^+, 2 e^-/2 H^+, 3 e^-/3 H^+, etc. Redox couples having slopes of −118 mV/pH unit involve an electron/proton ratio of 1/2, e.g., 1 e^-/2 H^+, 2 e^-/4 H^+, ..., and a slope of −30 mV/pH unit indicates an electron/proton ratio of 2 e^-/1 H^+. A slope of 0 mV/pH unit means that the redox process is pH-independent. The break points or changes in slope that appear in the $E_{1/2}$ vs. pH plots occur due to changes in the proton compositions of the complexes and give approximate pK_a values as shown by the vertical lines.[19] However, the Nernst equation applies to reversible systems so deviations of the measured slopes from ideal values may occur in quasi-reversible and irreversible systems. Also, since the variations in proton contents of the complexes are gradual, some curvature in the $E_{1/2}$–pH plots are expected near the break points.[19]

In the region $0.5 < pH < 2.2$ the slope of the $E_{1/2}$ vs. pH plot for the Re(V/III) couple is −90 mV/pH unit (2 e^-/3 H^+) and −60 mV/pH unit for Re(III/II) (1 e^-/1 H^+), showing that the couples are

$$[(py)_4Re^{V}(O)_2]^+ + 2e^- + 3H^+ \rightarrow [(py)_4Re^{III}(OH)(OH_2)]^{2+}$$

$$[(py)_4Re^{III}(OH)(OH_2)]^{2+} + e^- + H^+ \rightarrow [(py)_4Re^{II}(OH_2)_2]^{2+}$$

At pH 2.2, pK_{a2} is reached for Re(III), and in the region $2.2 < pH < 4.0$ the couples are

$$[(py)_4Re^{V}(O)_2]^+ + 2e^- + 2H^+ \rightarrow [(py)_4Re^{III}(OH)_2]^+ \text{ (or } [(py)_4Re(O)(OH_2)]^+)$$

$$[(py)_4Re^{III}(OH)_2]^+ + e^- + 2H^+ \rightarrow [(py)_4Re^{II}(OH_2)_2]^{2+}$$

as shown by the slopes of −60 and −120 mV/pH unit for Re(V/III) and Re(III/II).

At pH 4, pK_{a1} is reached for $[(py)_4Re^{II}(OH_2)_2]^{2+}$. As shown by the slope of −60 mV/pH unit, in the region $4.0 < pH < 6.0$, the Re(III/II) couple is

$$[(py)_4Re^{III}(OH)_2]^+ + e^- + H^+ \rightarrow [(py)_4Re^{II}(OH)(OH_2)]^+$$

At pH 6 the decrease in slope for the Re(V/III) couple shows that pK_{a3} has been reached for Re(III). Past pH >6.0, the slopes are −30 mV/pH unit for Re(V/III) and −120 mV/pH unit for Re(III/II) and the couples are

$$[(py)_4Re^{V}(O)_2]^+ + 2e^- + H^+ \rightarrow [(py)_4Re^{III}(O)(OH)]$$

$$[(py)_4Re^{III}(O)(OH)] + e^- + 2H^+ \rightarrow [(py)_4Re^{II}(OH)(OH_2)]^+$$

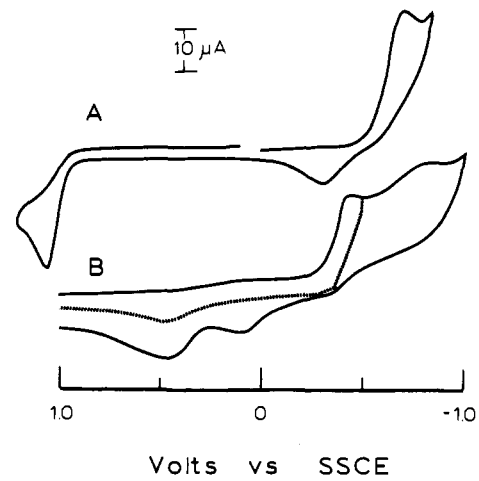

Figure 4. Cyclic voltammograms (100 mV/s) in aqueous solutions (0.1 M (TFMS)H) with oxidatively activated glassy-carbon working electrodes[20] vs. SSCE: (A) $[(en)_2Re^{V}(O)_2]^+$; (B) $[(CN)_4Re^{V}(O)_2]^{3-}$.

The pH dependence of the Re(V/III) couple remains the same throughout the remainder of the pH range, although past pH 7.0 the couple is more appropriately written as

$$[(py)_4Re^{V}(O)_2]^+ + 2e^- + H_2O \rightarrow [(py)_4Re^{III}(O)(OH)] + OH^-$$

pK_{a2} is reached for Re(II) at pH 7.1, and at $7.1 < pH < 8.7$, the Re(III/II) couple is

$$[(py)_4Re^{III}(O)(OH)] + e^- + H_2O \rightarrow [(py)_4Re^{II}(OH)_2] + OH^-$$

At pH 8.7 pK_{a3} for Re(II) is reached, and over the remainder of the pH range, $8.7 < pH < 13$, the Re(III/II) couple is pH-independent:

$$[(py)_4Re^{III}(O)(OH)] + e^- \rightarrow [(py)_4Re^{II}(O)(OH)]^-$$

Electrochemistry of $[(en)_2Re^{V}(O)_2]^+$ and $[(CN)_4Re^{V}(O)_2]^{3-}$. Although not studied in detail, the electrochemical properties of the Re(V)–dioxo complexes $[(en)_2Re^{V}(O)_2]^+$ and $[(CN)_4Re^{V}(O)_2]^{3-}$ were investigated by cyclic voltammetry in aqueous solutions. As shown in Figure 4, for $[(en)_2Re^{V}(O)_2]^+$ an irreversible oxidation occurs at $E_{p,a}$ = 1.06 V at an activated-glassy-carbon working electrode[20] at pH 1.0. Oxidation of $[(CN)_4Re^{V}(O)_2]^{3-}$ at pH 6.8 occurs with a broad, irreversible oxidation wave at $E_{p,a}$ = 1.4 V. Reduction of $[(en)_2Re^{V}(O)_2]^+$ occurs via a quasi-reversible wave at $E_{1/2}$ = −0.52 V (ΔE_p = 400 mV) at pH 1.0, which is probably a Re(V) to Re(III) wave. It was not possible to determine *n* for the wave by coulometry because of the electrocatalytic production of H_2 by the complex in its reduced form. The reduction of $[(en)_2Re^{V}(O)_2]^+$ is pH-dependent. For the apparent two-electron wave, $E_{1/2}$ values at different pH values were as follows: pH 5.4, $E_{1/2}$ = −0.91 V; pH 6.8, $E_{1/2}$ = −0.99 V; pH 11.1, $E_{1/2}$ = −1.19 V.

Reduction of $[(CN)_4Re^{V}(O)_2]^{3-}$ in 0.1 M (TFMS)H (pH 1.0) is chemically irreversible at least past the second wave. As shown in Figure 4B a reductive scan past the second wave gives a new product at $E_{p,a}$ = 0.45 V.

A comparison amongst the three complexes at pH 1.0 is made in Table II. In all cases oxidation to Re(VI) leads to coordinative instability with only $[(py)_4Re^{VI}(O)_2]^{2+}$ being stable on the cyclic voltammetry time scale. Reductively, $[(py)_4Re^{V}(O)_2]^+$ and $[(en)_2Re^{V}(O)_2]^+$ are quite similar with the Re(V/III) reduction for the bis(ethylenediamine) complex occurring at a more negative potential, $E_{1/2}$ = −0.43 V compared to −0.52 V. The ~100-mV offset in potential is apparently sufficient to make the Re(III)

(19) Bard, A. S.; Faulkner, L. R. *Electrochemical Methods*; Wiley: New York, 1980.

(20) Cabaniss, G. E.; Diamantis, A. A.; Murphy, W. R., Jr.; Linton, R. W.; Meyer, T. J. *J. Am. Chem. Soc.* **1985**, *107*, 1895.

Table II. Reduction Potentials (V vs. SSCE) for Re-Based Couples at pH 1.0 (CF_3SO_3H)[a]

complex	$E_{1/2}$ (VI/V)	$E_{1/2}$ (V/III)	$E_{1/2}$ (III/II)
trans-$[(py)_4Re^V(O)_2]^+$	1.25	~−0.43[b]	−0.75
trans-$[(en)_2Re^V(O)_2]^+$	1.06[c]	~−0.52[b]	
trans-$[(CN)_4Re^V(O)_2]^{3-}$	1.4[c,d]	−0.45[e]	−0.83[e]

[a] Glassy-carbon working electrodes. [b] Quasi-reversible waves; at a sweep rate of 100 mV/s, ΔE_p = 100 mV for $[(py)_4Re^V(O)_2]^+$ and ΔE_p = 400 mV for $[(en)_2Re^V(O)_2]^+$. [c] $E_{p,a}$ value at 100 mV/s sweep ratio. [d] Very broad wave. [e] $E_{p,c}$ value at 100 mV/s sweep rate for an irreversible wave; see Figure 4.

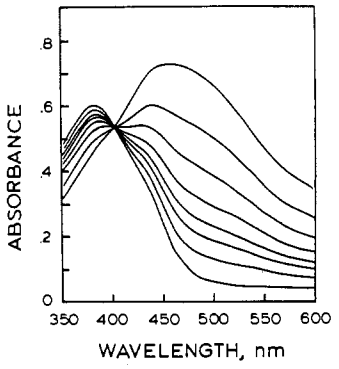

Figure 5. Visible absorbance changes in the reduction of H_2O at pH 1.2 (μ = 0.1 M (TFMS)H) by $[(py)_4Re^{II}(OH_2)_2]^{2+}$ (λ_{max} = 458 nm) to give $[(py)_4Re^{III}(OH)(OH_2)]^{2+}$, λ_{max} = 383 nm, [Re] = 8.2 × 10^{-5} M.

$(en)_2$ complex a catalyst for H_2O reduction. In the tetrakis(pyridine) system, a further reduction to Re(II) is required before H_2O reduction occurs at a noticeable rate. For the $(en)_2$ system, the appearance of the electrocatalytic reduction past the Re(V/III) wave may mask a further reduction of Re(III) to Re(II). An obvious alternative is that reduction at $E_{p,c}$ = 0.72 V occurs by a three-electron reduction of Re(V) to Re(II), which might also account for the H_2O reduction capability. The apparent Re(V/III) wave is sufficiently ill-defined and quasi-reversible that a Re(III/II) wave, even if reversible, could be hidden within the broad wave for the apparent two-electron reduction.

Reduction of H_2O to H_2 by Re(II). Electrocatalytic reduction of *trans*-$[(py)_4Re^V(O)_2]^+$ to Re(II) in solutions at pH 1.0, 6.8, and 13 produces H_2 as shown by gas chromatographic analysis. Comparison of coulometric results for the electrocatalyzed reductions to the number of moles of H_2 produced gives a ratio of ~2/1. The current efficiency ([(number of moles of H_2 produced)/$(n/2)$] × 100) was ≥87% at all three pH values. In the coulometric experiments sustained currents were obtained for times greater than 40 min without current loss. As the electrolyses proceeded, the pH increased as expected for H_2 production via

$$2H^+ + 2e^- \rightarrow H_2$$

or

$$2H_2O + 2e^- \rightarrow H_2 + 2OH^-$$

Kinetic studies of the rate of H_2 production were complicated by the difficulty of generating solutions containing Re(II) on a time scale that was short compared to the rate of H_2 evolution. Kinetic studies were carried out in (TFMS)H (pH 1.2) by generating $[(py)_4Re^{II}(OH_2)_2]^{2+}$ either by electrochemical means or by Zn(Hg) reduction. The spectral changes that occur were monitored from 600 to 350 nm; an example is shown in Figure 5, where the maintenance of the isosbestic point at λ = 398 nm throughout the reaction is notable. Absorbance changes (458 nm) vs. time followed first-order kinetices over $2^1/_2$–3 half-lives with k_{obsd} = 2.4 (±1.5) × 10^{-3} s^{-1} at room temperature. We were unable to carry out kinetics studies at pH 6.8 or 13, but it seems clear that the rates of water reduction at least parallel the driving forces for the reduction of H_2O at the different pH values. $E_{1/2}$ values for the Re(III/II) couples (vs. SSCE) and electrochemical

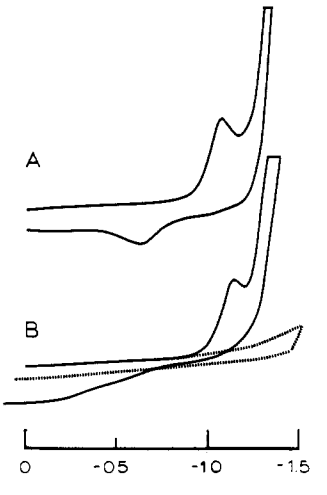

Figure 6. Cyclic voltammograms (100 mV/s) in aqueous solutions (pH 6.8, μ = 0.1 M (phosphate)) of *trans*-$[(py)_4Re^V(O)_2]^+$ at glassy-carbon working electrodes in the presence of (A) 0.1 M $NaNO_2$ and (B) 0.1 M Na_2SO_3. The dashed line indicates the CV observed in the absence of the Re complex; the current scale is the same as in Figure 4.

driving forces ($E^{\circ\prime}$) for the net reactions as a function of pH are as follows: (a) pH 1.0, $E_{1/2}$ = −0.75 V, $E^{\circ\prime}$ = 0.45 V; (b) pH 6.8, $E_{1/2}$ = −1.28 V, $E^{\circ\prime}$ = 0.68 V; (c) pH 13, $E_{1/2}$ = −1.40 V, $E^{\circ\prime}$ = 0.39 V.

Qualitatively, reduction of $[(en)_2Re^V(O)_2]^+$ past $E_{p,c}$ = −0.72 V at pH 1 results in a considerable electrocatalytic current enhancement compared to reduction of $[(py)_4Re^V(O)_2]^+$ past the Re(III/II) wave at −0.75 V under the same conditions. The effectiveness of the $(en)_2$ complex as a catalyst reinforces the possibility mentioned earlier that the Re(III/II) couple may be hidden within a multielectron reduction wave and Re(II) may be the active catalytic oxidation state here as well.

Reduction of NO_2^- and SO_3^{2-}. Cyclic voltammograms of $[(py)_4Re(O)_2]^+$ in the presence of NO_2^- or SO_3^{2-} (Figure 6) at 100 mV/s show catalytic current enhancement well above background at pH 6.8 but not at pH 13. That electrocatalytic reduction occurs at both pH values is shown by both coulometry and product analyses. In acidic solutions direct reduction of HONO or SO_2 is sufficiently facile to mask the Re(III/II) electrocatalysis. In the coulometry experiments the initial current dropped ~50% during the first 10–15 min of the electrolysis period and then decreased very slowly over the remaining period. The initial current was higher at pH 6.8 than at pH 13 but dies off more rapidly at pH 6.8. The more rapid loss of current at pH 6.8 is attributable to a greater stability (toward pyridine loss) at pH 13 and, in the case of NO_2^-, to slow decomposition of the catalyst induced by added NO_2^-.

After coulometry in the presence of NO_2^- both the gas and liquid phases were analyzed by GLC and GC. The solution contained significant amounts of NH_3 and N_2O. Only small amounts of H_2 were detected at either pH, showing that in the presence of NO_2^- the reduction of H_2O is greatly suppressed.

In the reduction of SO_3^{2-}, the current decreased significantly after approximately 25 min of electrolysis and a suspension appeared in the solution. The suspension was a sulfide, presumably ReS_2 or a "(py)ReS" complex given the partial loss of catalyst as shown by the cyclic voltammetry. Attempts to preserve the catalyst by capturing S^{2-} as produced by the formation of insoluble ZnS or CdS by the addition of Zn^{2+} or Cd^{2+} were unsuccessful.

Discussion

Redox Properties. Examination of the Pourbaix diagram in Figure 3 shows that over the pH range pH 0 to pH 14 the Re(V/III) two-electron couple persists without evidence for the appearance of one-electron Re(V/IV) or Re(IV/III) couples. By inference, Re(IV) is unstable with respect to disproportionation

$$2Re(IV) \rightarrow Re(III) + Re(V)$$

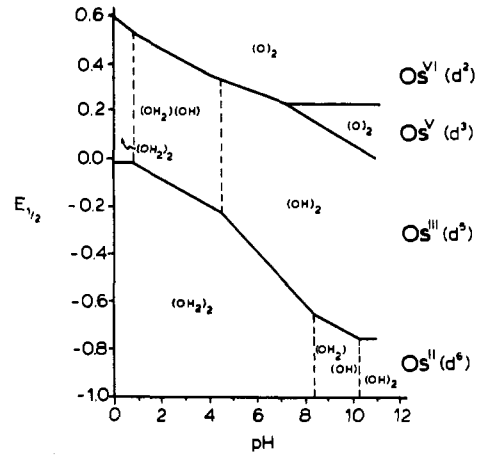

Figure 7. Pourbaix diagram ($E_{1/2}$ vs. pH) for *trans*-$[(bpy)_2Os^{VI}(O)_2]^{2+}$.[9b]

over the entire pH range. It also follows that (1) $E^{\circ\prime}$(Re(IV/III) > $E^{\circ\prime}$(Re(V/IV) and Re(IV) is a stronger oxidant than Re(V) and (2) the experimental value for the Re(V/III) couple is the average of the potentials for the Re(V/IV) and Re(IV/III) couples

$$E^{\circ\prime}(\mathrm{Re(V/III)}) = \tfrac{1}{2}[E^{\circ\prime}(\mathrm{Re(IV/III)}) + E^{\circ\prime}(\mathrm{Re(V/IV)})]$$

The appearance of multielectron couples is a common occurrence for metal–aqua/oxo complexes. They appear, for example, for *cis*- and *trans*-$[(bpy)_2M^{VI}(O)_2]^{2+}$,[8] $[(trpy)Os^{VI}(O)_2(OH)]^+$,[21] and $[(cat)Mo^{VI}(O)_2]^{2-}$.[9] The bases for oxidation-state instability have been discussed elsewhere.[8d,17,21b] They include electronic effects and simple differences in pH dependences between adjacent couples.

From the fundamental point of view the most interesting feature to arise from this work is the ability to make comparisons between the redox properties of complexes of different metals in the same or nearly the same coordination environments. The most apt comparison is with *trans*-$[(bpy)_2Os^{VI}(O)_2]^{2+}$, where, although there is a slight difference in the coordination environment, the d-electronic configuration is the same (d^2) as is the trans stereochemistry at the metal. The Pourbaix diagram for the Os complex is shown in Figure 7.

When they are viewed carefully, there is a remarkable similarity in the redox characteristics of the two systems. In both cases the potentials for the three couples that interrelate d^2–d^5 Re(V) and Re(II) or Os(VI) and Os(III) occur within a span of ≤0.5 V. In that sense the pattern of redox couples appears to be dictated by the d-electronic configurations that make up the couples. However, the lower oxidation states for the analogous Re couples shift potentials negatively by greater than 1 V.

In finer detail there are interesting differences between the d^2–d^5 Re and Os couples. For Os(VI/III), electronic stabilization of Os(VI) by the *trans*-dioxo group lowers the potential of the Os(VI/V) couple below Os(V/III) and Os(IV/III) and only the 3e Os(VI/III) couple is observed.[8d] Although the Os(VI/V) and two-electron Os(V/III) couples appear past pH > 7 because of the difference in pH dependences between the two couples, d^4 Os(IV) is not observed as a stable oxidation state over the entire pH range. For Re, *trans*-dioxo stabilization decreases the potential of the Re(V/IV) couple below that of the Re(IV/III) couple and only the Re(V/III) couple is observed over the entire pH range. One important difference between Re and Os is that d^4 Re(III) appears to be stabilized relative to d^4 Os(IV). As a consequence, the potential of the Re(V/III) couple is always well above that of the Re(III/II) couple, d^4 Re(III) is a stable oxidation state over the entire pH range, and a 3e (Re(V/IV) couple does not appear.

The effect of oxidation state on potentials for couples having equivalent d-electronic configurations also dictates which oxidation states appear within the solvent limits. At electron-rich Re, the pH-independent d^1/d^2 Re(VI/V) couple $[(py)_4Re^{VI}(O)_2]^{2+}/[(py)_4Re^{V}(O)_2]^{+}$ is observed at +1.25 V but there is no evidence for the analogous Os(VII/VI) couple $[(bpy)_2Os^{VII}(O)_2]^{3+}/[(bpy)_2Os^{VI}(O)_2]^{2+}$. If the ~1.0 V potential difference between the Re(V/II) and Os(VI/III) couples were maintained in the Re(VI/V) and Os(VII/VI) couples, the Os couple lies past the solvent limit at ~2.3 V but may be observable, for example, in liquid SO_2, where the solvent limit is >3 V.[19,22] On the other hand, at Os, which is more electron-deficient, the d^5/d^6 Os(III/II) couple appears over the entire pH range but the analogous d^5/d^6 Re(II/I) couple is not observed. At pH 13 the potential for *trans*-$[(bpy)_2Os(OH)_2]^{2+/+}$ is −0.76 V, which is ~0.8 V below the Os(VI/III) couple. Assuming that the same separation is maintained for Re would place the Re(II/I) couple at ~−2.0 V. Note from the data in Figure 2c that in the cyclic voltammogram of *trans*-$(py)_4Re^{V}(O)_2^{+}$ at pH 13.0 a shoulder is observed on the solvent background wave at $E_{p,c}$ = −1.7 V. Its origin may be in a Re(II/I) couple.

Table III. Acid/Base Properties at 23 ± 1 °C and μ = 0.1 M[a]

complex	d-electronic confign	$pK_{a,1}$	$pK_{a,2}$	$pK_{a,3}$
trans-$[(py)_4Re^{III}(OH_2)_2]^{3+}$	d^4	<0	2.2	6.0
trans-$[(py)_4Re^{II}(OH_2)_2]^{2+}$	d^5	4.0	7.1	8.7
trans-$[(bpy)_2Os^{III}(OH_2)_2]^{3+}$	d^5	0.5	4.4	>14
trans-$[(bpy)_2Os^{II}(OH_2)_2]^{2+}$	d^6	8.2	10.2	>14
cis-$[(bpy)_2Os^{III}(OH_2)_2]^{3+}$	d^5	1.9	5.4	>14
cis-$[(bpy)_2Os^{II}(OH_2)_2]^{2+}$	d^6	7.8	11.0	>14

[a] Data for the cis and trans Os complexes from ref 8d.

Acid/Base Properties. In Table III are listed pK_a values for the Re(III) and Re(II) diaqua complexes derived from *trans*-$[(py)_4Re^{V}(O)_2]^{+}$ and, for comparison, values obtained for analogous cis and trans 2,2′-bpy complexes of Os(II) and Os(III). The values were obtained from the breaks in the $E_{1/2}$ vs. pH plots in Figure 3. In earlier work on Ru and Os aqua complexes, pK_a values obtained from pH-dependent electrochemical data were in good agreement with values obtained from spectrophotometric or potentiometric titrations.[8,17,21]

From the data in Table III, comparisons of pK_a values for the same oxidation state show that Re(III) and Re(II) are considerably more acidic than Os(III) and Os(II) and that they have three rather than two dissociable protons over the accessible pH range. In comparisons involving complexes of the types $(bpy)_2Os^{III/II}$ and $(py)_4Re^{III/II}$, the complexes have the same charge type and approximately the same molecular volumes so that solvation energies should be nearly the same. If solvation energies are nearly constant, variations in pK_a values are a direct measure of the differences in gas-phase acidities between analogous complexes of Re and Os and, therefore, of electronic effects associated with proton gain or loss.

The greater acidities of the Re complexes having the same charge types show that electronic effects stabilize the conjugate bases of Re to a greater extent than those of Os. A quantitative estimate of the effect can be calculated from the ratio of pK_a values for equivalent complexes in Table III by $\Delta(\Delta G) = -RT \ln (K_a(\mathrm{Re})/K_a(\mathrm{Os}))$. From the pK_a ratios the following differential electronic stabilization energies for Re can be calculated: *trans*-$[(L)_4M^{III}(O)(OH_2)]^{2+}$, −0.13 V; *trans*-$[(L)_4M^{II}(OH)(OH_2)]^{+}$, −0.25 V; *trans*-$[(L)_4M^{II}(OH)_2]$, −0.18 V.

The greater electronic stabilization for Re (−0.13 to −0.25 V) suggests that $p\pi(O^{2-}$ or $OH^-)$ to $d\pi$ mixing is more important for Re(III) than for Os(III) and for Re(II) compared to Os(II). This is, no doubt, another consequence of the difference in electronic configurations between oxidation states. For d^4 Re(III) the capability for metal–oxo formation exists in $[(L)_4Re^{III}(O)(OH_2)]^{+}$, while for d^5 Os^{III}, the dominant form may be the compositionally equivalent dihydroxo complex $[(L)_4Os^{III}(OH)_2]^{+}$. For d^5 Re(II), $p\pi(OH^-)$ to $d\pi$ back-bonding is possible, but for d^6 Os(II), the $d\pi$ levels are filled.

(21) (a) Pipes, D. W.; Meyer, T. J. *J. Am. Chem. Soc.* **1984**, *106*, 7653. (b) Pipes, D. W.; Dobson, J. C.; Meyer, T. J. *Inorg. Chem.*, in press.

(22) Gaudiello, J. G.; Bradley, P. G.; Norton, K. A.; Woodruff, W. H.; Bard, A. J. *Inorg. Chem.* **1984**, *23*, 3.

For complexes having the same d-electronic configuration but different oxidation states, d^5 Re(II) vs. d^5 Os(III), the higher oxidation state is more acidic as would be expected on the basis of its comparatively more "electron deficient" character. However, a distinctive feature of the Re(II) complex is the loss of a third proton at $pK_a = 8.7$, which is *not* observed for Os(III), to give the d^5 oxo complex $[(py)_4Re^{II}(O)(OH)]^-$. Attempts to isolate this anion by electrochemical generation in 0.1 M NaOH and addition of tetra-*n*-butylammonium nitrate or tetraphenylarsonium chloride were unsuccessful due to the solubility and reactivity toward solvent reduction of the reduced form. Because of the loss of the third proton, the Re(III/II) redox couple becomes pH-independent at pH >8.7. A similar observation has been made in the aqueous electrochemistry of $(phen)Os^{VI}(O)_2(OH)_2$ (phen is 1,10-phenanthroline), where the d^4/d^5 Os(IV/III) couple also becomes pH-independent at pH >8.7, suggesting the possibility of oxo formation in the d^5 Os(III) complex as well.[21b]

Chemical Reactivity. Although *trans*-$[(py)_4Re^V(O)_2]^+$ shares with *cis*- and *trans*-$[(bpy)_2Os^{VI}(O)_2]^{2+}$ an extensive multiple-electron-transfer chemistry, the potentials for the Re couples are lower by >1 V. The utilization of oxo complexes of Ru and, to a lesser extent, of Os as multielectron oxidants vis H atom, hydride, or O atom transfer pathways was mentioned in the Introduction. One of the intentions of the present work was to begin the development of lower oxidation state Re(III) and Re(II) complexes as multielectron reductants possibly by utilizing the microscopic reverse of known oxidation pathways based on Ru and Os:

$$M^{IV}{=}O + (CH_3)_2C(H)OH \underset{(?)}{\overset{M = Ru(IV)}{\underset{M = Re(II,III)}{\rightleftharpoons}}} M^{II}OH_2 + (CH_3)_2C{=}O$$

$$M^{IV}{=}O + NO_2^- + H_2O \underset{(?)}{\overset{M = Ru(IV)}{\underset{M = Re(II,III)}{\rightleftharpoons}}} M^{II}OH_2 + NO_3^-$$

The results we have obtained for the Re(II) or Re(III) complexes as stoichiometric or electrocatalytic reductants are mixed. Attempts to observe reductive current enhancements for the Re(V/III) or Re(III/II) couples at pH 1, 6.8, or 13 in the presence of ClO_4^-, NO_3^-, or SO_4^{2-} were unsuccessful. Although slow reductions by Re(II) may have been masked by reduction of H_2O, for Re(III) there is no obvious indication of a reaction with any of the anions. The attempted electrocatalytic reduction of acetone to isopropyl alcohol by either Re(II) or Re(III) was also unsuccessful.

The anions NO_2^- and SO_3^{2-} are reduced by Re(II) as shown by the current-enhanced cyclic voltammograms in Figure 6 and coulometry. Although reduction of SO_3^{2-} was complicated by decomposition of the Re complex, sulfide was detected as a reduction product. The reduction of NO_2^- is catalytic at pH 6.8 or 13, and NH_3 and N_2O were detected by GC as major reduction products.

The appearance of current enhancement of the Re(III) → Re(II) wave in the presence of NO_2^- or SO_3^{2-} suggests that they bind rapidly, a conclusion that is reinforced by the suppression of the reduction of H_2O to H_2 at pH 6.8, for which $k_{obsd} > 10$ s^{-1}. A similar observation has been made for $[(cat)_2Mo^{VI}(O)_2]^{2-}$ by Lahr, Finklea, and Schultz in that electrochemical reduction to Mo(III) leads to reduction of the oxo anions, NO_2^-, ClO_3^-, and BrO_3^- but not of ClO_4^-.[9] For polypyridyl complexes of Ru and Os there is a high affinity for NO_2^- and the mechanistic details of the reduction of bound NO_2^- to NH_3 include a series of one-electron, proton-coupled steps,[23] and the mechanistic details for Re may be similar.

The imprecision of the kinetics data for H_2O reduction prevented a detailed investigation of the mechanism. However, some of our observations are worthwhile. The rate of H_2 production is first order in Re(II) in acidic solutions (pH 1.2). Because of experimental complications the pH dependence was not determined. However, the reduction of H_2O by Re(II) is considerably more rapid as pH 6.8 ($k_{obsd} > 10$ s^{-1}) than at pH 1.2 ($k_{obsd} = 2.5 \times 10^{-3}$ s^{-1}), suggesting at least an inverse proton dependence in this region. The reaction slows down again as the pH is increased, and at pH 13, $k_{obsd} \approx 10^{-3}$ s^{-1}.

In previous work on water reduction, the mechanism of reduction by $[(bpy)_2CoH(OH_2)]^{2+}$ was shown to be complex,[24] cobalt and rhodium hydride complexes were shown to reduce water,[25] and, recently, Spiro and Kellet have studied the electrocatalytic reduction of H_2O by cobalt porphyrins.[26] Although no evidence for formation of a rhenium hydride intermediate has been obtained here, even a small but reactive amount at equilibrium could control the observed reactivity. Low-oxidant-state complexes containing the Re–H group are known, for example, $(PPh_3)_3ReH_5$, $(dppe)_2(CO)ReH$, and $(\eta\text{-}C_5H_5)_2ReH$,[27] and the reduction of the dioxo complex $[(en)_2Os^{VI}(O)_2]^{2+}$ has been reported to give a dihydride:[28]

$$[(en)_2Os^{VI}(O)_2]^{2+} \xrightarrow{Zn/Hg,\ H_2O} [(en)_2Os^{IV}(H)_2]^{2+}$$

Acknowledgements are made to the National Science Foundation under Grant No. CHE-8304230 and to the National Institutes of Health under Grant No. 5-RO1-GM32296-03 for support of this research.

Registry No. *trans*-$[(py)_4Re^V(O)_2]^+$, 21710-28-1; $[(py)_4Re^{III}(OH)(OH_2)]^{2+}$, 103191-74-8; $[(py)_4Re^{II}(OH_2)_2]^{2+}$, 99268-99-2; $[(py)_4Re^{III}(OH)_2]^+$, 103191-75-9; $[(py)_4Re^{III}(O)(OH)]$, 103191-76-0; $[(py)_4Re^{II}(OH)(OH_2)]^+$, 99269-00-8; $[(py)_4Re^{II}(O)(OH)]^-$, 99269-01-9; *trans*-$[(en)_2Re^V(O)_2]^+$, 21602-78-8; *trans*-$[(CN)_4Re^V(O)_2]^{3-}$, 20756-46-1; *trans*-$[(py)_4Re^{III}(OH_2)_2]^{3+}$, 103191-77-1; *trans*-$[(py)_4Re(O)_2](ClO_4)$, 83311-31-3; $[(py)_4Re^{VI}(O)_2]^{2+}$, 99269-02-0; H_2O, 7732-18-5; NO_2^-, 14797-55-8; SO_3^{2-}, 14265-45-3; HSO_3CF_3, 1493-13-6; H_2, 1333-74-0.

(23) (a) Murphy, W. R., Jr.; Takeuchi, K. J.; Meyer, T. J. *J. Am. Chem. Soc.* **1982**, *104*, 5817. (b) Murphy, W. R., Jr.;, Takeuchi, K.; Barley, M. H.; Meyer, T. J. *Inorg. Chem.* **1986**, *25*, 1041.
(24) Creutz, C.; Sutin, N.; Schwarz, H. A. *J. Am. Chem. Soc.* **1984**, *106*, 3036.
(25) (a) Espenson, J. H.; Chao, T.-H. *J. Am. Chem. Soc.* **1978**, *100*, 129. (b) Espenson, J. H.; Ramasami, T. *Inorg. Chem.* **1980**, *19*, 1846.
(26) Spiro, T. G.; Kellet, R. M. *Inorg. Chem.* **1985**, *24*, 2373.
(27) (a) DeVries, B. *J. Catal.* **1962**, *1*, 489. (b) Burnet, M. G.; Connolly, P. J.; Kembal, C. *J. Chem. Soc. A* **1967**, 800.
(28) Malin, J. M.; Taube, H. *Inorg. Chem.* **1971**, *10*, 2403.